

Prediction of Stable Ground-State Binary Sodium-Potassium Interalkalis under High Pressures

Yangmei Chen¹, Xiaozhen Yan^{1,2}, Huayun Geng*², Xiaowei Sheng³, Leilei Zhang²,*

Hao Wang², Jinglong Li², Ye Cao,² and Xiaolong Pan²

1. School of Science, Jiangxi University of Science and Technology, Ganzhou

341000, Jiangxi, People's Republic of China

2. National Key Laboratory of Shock Wave and Detonation Physics, Institute of

Fluid Physics, CAEP, P.O. Box 919-102, Mianyang 621900, Sichuan, People's

Republic of China

3. Department of Physics, Anhui Normal University, Anhui 241000, Wuhu, People's

Republic of China

Corresponding Author

* Xiaozhen Yan: xzyan01@qq.com.

* Huayun Geng: s102genghy@caep.cn.

ABSTRACT The complex structures and electronic properties of alkali metals and their alloys provide a natural laboratory for studying the interelectronic interactions of metals under compression. A recent theoretical study (*J. Phys. Chem. Lett.* **2019**, 10, 3006) predicted an interesting pressure-induced decomposition-recombination behavior of the Na₂K compound over a pressure range of 10 - 500 GPa. However, a subsequent experiment (*Phys. Rev. B* **2020**, 101, 224108) reported the formation of NaK rather than Na₂K at pressures above 5.9 GPa. To address this discordance, we study the chemical stability of different stoichiometries of Na_xK ($x = 1/4, 1/3, 1/2, 2/3, 3/4, 4/3, 3/2$ and 1 - 4) by effective structure searching method combined with first-principles calculations. Na₂K is calculated to be unstable at 5 - 35 GPa due to the decomposition reaction $\text{Na}_2\text{K} \rightarrow \text{NaK} + \text{Na}$, coinciding well with the experiment. NaK undergoes a combination-decomposition-recombination process accompanied by an opposite charge-transfer behavior between Na and K with pressure. Besides NaK, two hitherto unknown compounds NaK₃ and Na₃K₂ are uncovered. NaK₃ is a typical metallic alloy, while Na₃K₂ is an electride with strong interstitial electron localization.

KEYWORDS. Alkali metals; Structure search; First-principles calculation; Crystal structure; Electronic property.

■ INTRODUCTION

The alkali metals with single valence electron configuration are considered textbook examples of electronic structures of metals. At ambient conditions, the quasifree valence electron leads to simple atomic bonding and highly symmetric bcc structures. On modest compression, they retain their free-electron-like behavior and transform to a more close-packed fcc structure. Under further compression, all alkalis undergo phase transitions from fcc to complex structures¹⁻¹¹ accompanied by a decrease in symmetry, coordination number and packing density.

From the energy-band theory, the pressure induced $s \rightarrow p$ and $s \rightarrow d$ charge transfer or hybridization is the key to comprehend the appearance of complex phases and properties.^{2-3, 12-13}

For the elemental alkali metals, increasing pressure results for Li and Na in $s \rightarrow p$ charge transfer,^{2, 5, 14-16} and for K, Rb and Cs $s \rightarrow d$ transfer.^{15, 17} Since the shapes of p and d orbitals are more complex, the p - and d -governed bonding are inevitably more complex, which therefore results in more complex structures, accompanied by remarkable physical phenomena such as enhanced superconductivity,¹⁸⁻²⁰ reduced melting temperatures,^{4, 21-22} and transformations into electride compounds.^{2, 21, 23-26}

For the binary combinations of alkali metals, the underlying charge transfer and redistribution of electrons between them, and the resultant properties have also attracted a lot of attention. An example is the Li-Cs alloy which is not formed at ambient conditions due to the large disparity in their atomic sizes. Theoretical calculations within density-functional theory (DFT) performed by Zhang et al.²⁷ reveal that

compressing can fundamentally alter the repulsive nature of Li and Cs, driving them to form intermetallic compounds LiCs and Li₇Cs at 160 GPa and 80 GPa, respectively. Analysis of valence charge density shows electron transfer from Cs to Li, resulting in oxidation states of Li. Botana et al.²⁸ predict by structure searching simulations and DFT calculations that Cs can gain electrons from Li, and to form stable compounds Li_nCs ($n = 1 - 5$) above 100 GPa. However, a subsequent diamond-anvil-cells (DAC) experiment performed by Desgreniers et al.²⁹ find that Li-Cs alloys could be experimentally synthesized at very low pressure (> 0.1 GPa).

Besides Li-Cs, compound formation has also been reported experimentally³⁰ in Na-Cs (Na₂Cs) and K-Cs (K₂Cs, K₇Cs₆) systems. The Na₂Cs and K₂Cs compounds in the MgZn₂-type Laves phase are calculated to have negative formation enthalpies within DFT.²⁷ The Li-Na system is predicted theoretically to form an insulating electride compound LiNa under 355 GPa.³¹ In the Na-K system, additionally, the eutectic NaK is a liquid alloy at room temperature and solidifies at 260 K, which is used as a coolant in nuclear reactors.³² When cooling down to 240 K under normal pressure, only the Na₂K solid is observed experimentally.³³ Theoretical calculations³⁴ confirm the stability of Na₂K in the MgZn₂-type Laves phase due to the negative enthalpy. It has also been suggested by limited experimental data on the formation of a NaK₂ intermetallic compound at high pressures; however, the existence of this compound has not yet been confirmed.³³

Most recently, Yang et al.³⁵ uncovered several new structures of Na₂K over a pressure range of 10 - 500 GPa, by swarm-intelligence structure-searching simulation.

Notably, this compound is predicted to undergoes a decomposition-recombination behavior with pressure. A subsequent DAC experiment³⁶ observed the formation of Na₂K at pressures below 5.9 GPa. Above this pressure, however, the Na-K system forms NaK instead of Na₂K up to at least 48 GPa, which is inconsistent with the theoretical prediction.

To gain further insight into the chemical stability of Na-K system, we perform extensive structure searches for different stoichiometric Na_xK ($x = 1/4, 1/3, 1/2, 2/3, 3/4, 4/3, 3/2$ and $1 - 4$) under high pressures. Our results reveal that NaK undergoes a combination-decomposition-recombination process with pressure. Na₂K is not stable with respect to NaK and Na. Instead, two ground-state stable phases of NaK₃ and Na₃K₂ are identified.

■ COMPUTATIONAL DETAILS

Our structural searching simulation is based on a global minimization of *ab initio* total-energy calculations as implemented in the CALYPSO (Crystal structure AnaLYsis by Particle Swarm Optimization) code,³⁷⁻⁴¹ which has demonstrated good efficiency in predicting high-pressure structures of pure alkali metals,^{24,42} alkali metal polyhydrides⁴³ and alkali alloys.^{28,31,35} Structure predictions of Na_xK ($x = 1/4, 1/3, 1/2, 2/3, 3/4, 4/3, 3/2$ and $1 - 4$) are performed at 100, 300 and 500 GPa, with $1 - 4$ formula units per simulation cell. Each search generation contains 30-50 structures and the structure searching simulation is usually stopped after generates 900-1500 structures. *Ab initio* structural relaxations and electronic structure calculations are carried out by using the Vienna ab-initio simulation package (VASP)⁴⁴ with the

Perdew-Burke-Ernzerhof (PBE) generalized gradient approximation (GGA) functional.⁴⁵ $2s^22p^63s^2$ of Na and $3s^23p^64s^1$ of K are treated as valence electrons for projected-augmented-wave pseudopotentials. The cut-off energy for the expansion of wavefunctions into plane waves is set to 950 eV in all calculations, and the Monkhorst-Pack grid with a maximum spacing of 0.02 \AA^{-1} is individually adjusted in reciprocal space to the size of each computational cell, which usually give total energies converged to ~ 1 meV per atom. Lattice dynamics is calculated by the small displacement method as implemented in the PHONOPY package.⁴⁶ The formation enthalpy (ΔH) of Na_mK_n with respect to elemental Na and K is calculated by using the following formula:

$$\Delta H(\text{Na}_m\text{K}_n) = [H(\text{Na}_m\text{K}_n) - mH(\text{Na}) - nH(\text{K})]/(m + n)$$

wherein H is the enthalpy of the most stable structure of certain compositions at the given pressure. For Na, the bcc, fcc, cI16, oP8, and hP4 structures were adopted^{2, 4, 10, 47-48}. And for K, the bcc, fcc, oP8, tI4, oC16, and hP4 structures were adopted⁴⁸⁻⁵⁰.

■ RESULTS AND DISCUSSION

The structure-searching results of Na_xK ($x = 1/4, 1/3, 1/2, 2/3, 3/4, 4/3, 3/2$ and $1 - 4$) at pressures of 100, 300 and 500 GPa are summarized in Figure 1a, wherein the phases located on the convex hull are chemically stable against any type of decomposition. It is apparent that no compounds considered here are stable at 100 GPa because of the positive formation enthalpies. At 300 GPa, NaK_3 and Na_3K_2 become stable, the other compounds NaK , NaK_2 , NaK_4 , Na_2K_3 and Na_3K_4 , as well as the previously predicted Na_2K^{35} are metastable due to their negative formation enthalpies but locating above the

convex hull. When pressure increases to 500 GPa, NaK₃ remains its stability, whereas Na₃K₂ is unstable upon decomposition into NaK and Na.

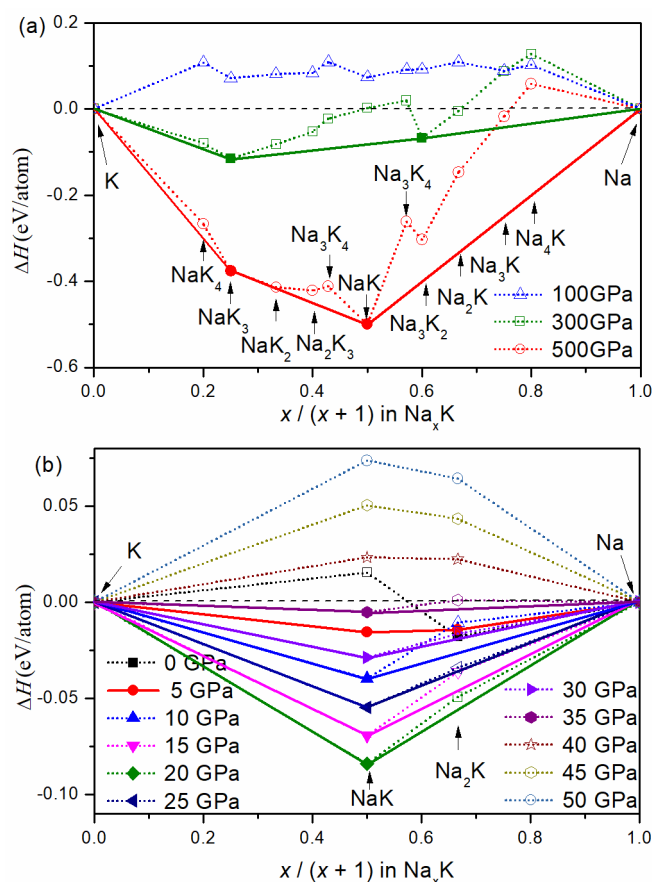


Figure 1. Chemical stabilities of Na-K system with respect to elemental Na and K at different pressures. (a) Chemical stabilities of various Na_xK compounds at 100 - 500 GPa (b) Chemically stabilities of NaK and Na_2K at 0 - 50 GPa. The stable phases are shown using solid symbols connected by solid lines on the convex hull.

For the simplest stoichiometry of NaK, our searches show that the energetically most favorable structures adopt the $Fd\bar{3}m$ symmetry at 100 and 300 GPa, and the $Ibmm$ at 500 GPa. As is shown in Figure 2a, the $Fd\bar{3}m$ structure is comprised of two interpenetrating diamond-type sublattices of Na and K. Both Na and K in this structure have a coordination number of 4. In the $Ibmm$ structure (Figure 2b), the coordination numbers of Na and K both increase to 8. The structural details at selected pressures for

$Fd\bar{3}m$ and $Ibmm$ phases are listed in Table S1 in the Supporting Information. Phonon calculations reveal no imaginary frequency in the phonon spectrums (Figure S1), implying that these structures are dynamically stable.

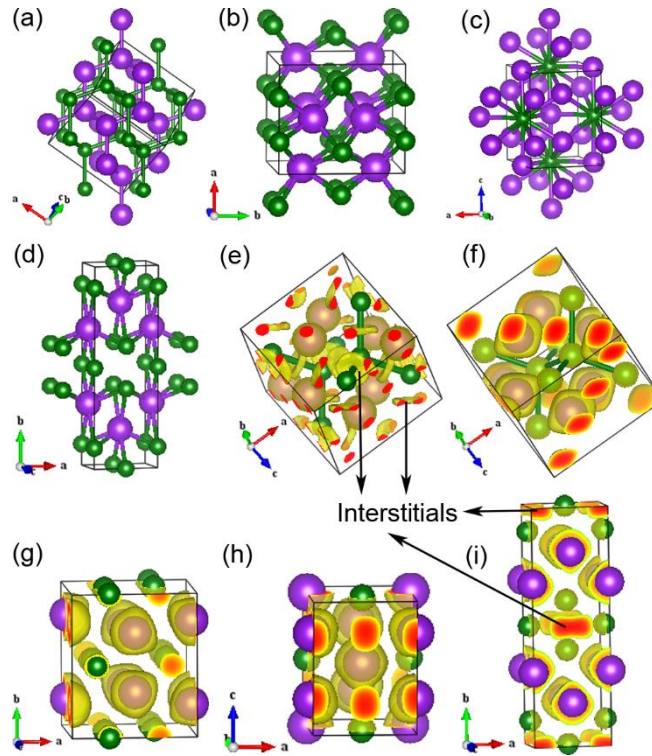


Figure 2. Crystal structures and bonding properties. Crystal structures of (a) $Fd\bar{3}m$ NaK, (b) $Ibmm$ NaK, (c) $Pnmm$ NaK₃ and (d) $Cmmm$ Na₃K₂; Electron localization function plots with isosurface of 0.6 for (e) $Fd\bar{3}m$ NaK at 10 GPa, (f) $Fd\bar{3}m$ NaK at 310 GPa, (g) $Ibmm$ NaK at 500 GPa, (h) $Pnmm$ NaK₃ at 300 GPa and (i) $Cmmm$ Na₃K₂ at 300 GPa. Green (small) and purple (large) spheres denote Na and K atoms, respectively.

As observed in the experiment,³⁶ the Na-K system forms Na₂K at 0 - 5.9 GPa. Above this pressure, however, it forms NaK instead of Na₂K up to at least 48 GPa. As revealed by our calculation, NaK becomes stable at a pressure approaches to 5 GPa (Figure 1b). At 35 GPa, it becomes unstable upon decomposition into Na and K. In the case of Na₂K, it remains stable at 0 - 5 GPa. Above this pressure, it is unstable due to the decomposition of Na₂K \rightarrow NaK + Na. Therefore, our results correspond well with the

experimental observation.³⁶ Moreover, when pressure further increases to 500 GPa, NaK comes back to the most stable phase on the convex hull (Figure 1a).

It is known that the formation enthalpy of a compound can be separated into two parts of contribution, the relative internal energy ΔU and the ΔPV term, i.e., $\Delta H = \Delta U + \Delta PV$. The pressure dependence of ΔU and ΔPV of NaK are plotted in Figure 3. Around 5 GPa, ΔU is calculated to be positive while ΔPV is negative. The negative ΔPV suggests that a better packing can be achieved in NaK than in elemental Na and K, which is responsible for its stability. As pressure increases to above 22 GPa, ΔPV becomes positive and the main contribution of the negative formation enthalpy comes from internal energy ΔU . However, as pressure increases to above 36 GPa (< 300 GPa), the negative ΔU is not enough to balance the increase in ΔPV , which leads to the decomposition due to the positive formation enthalpy. Furthermore, at pressures above 300 GPa, the formation enthalpy falls back to negative owing to the optimum structure-packing (relative to elemental Na and K) which results in negative ΔPV (Figure 3b).

In elemental alkali metals, the pressure induced $s \rightarrow p$ and $s \rightarrow d$ charge transfer or hybridization is the key to comprehend the appearance of complex phases and properties.^{2-3, 12} To get further insights into the physical origin of the formation of NaK, the nature of chemical bonding is then analyzed.

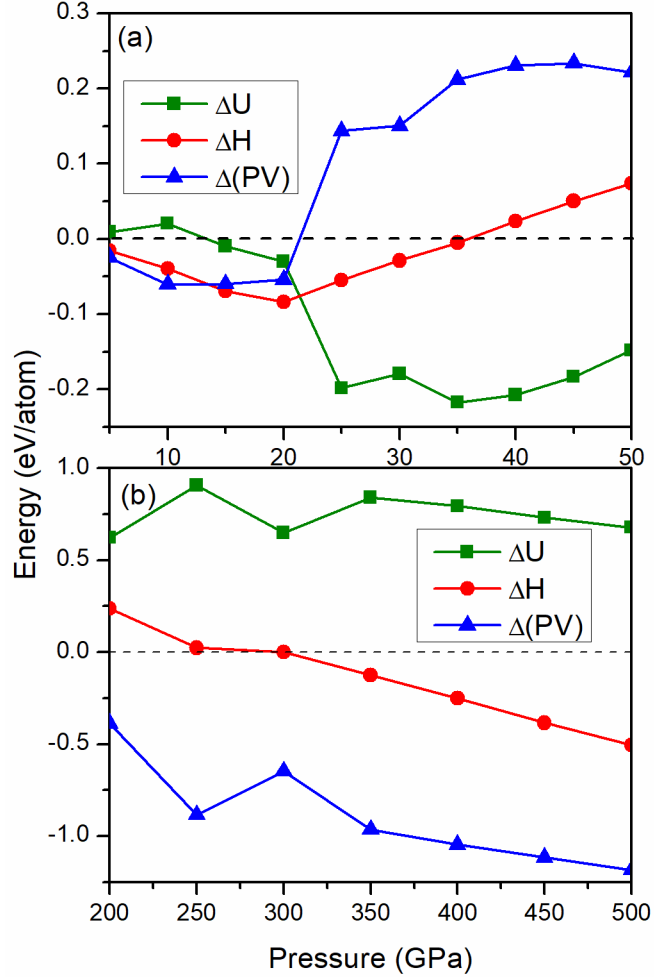


Figure 3. Relative changes in enthalpy H , the PV term, and internal energy U for NaK (a) at 5 - 50 GPa and (b) 200 - 500 GPa.

Our Bader charge analysis reveals that the charge-transfer directions between Na and K atoms in NaK are opposite below and above ~ 50 GPa (Figure S2). The pressure-induced charge reversal has also been found in Na_2K ³⁵. This behavior can be explained by the pressure-induced change in electronegativity of Na and K elements. According to the electronegativity data calculated by Dong et al⁵¹, under low pressures (< 50 GPa), Na element is more electronegative than K since the former has a smaller atomic size, and thus charge transfer from K to Na takes place; Under high pressures (> 50 GPa), K becomes a d -block element due to the pressure-induced $s \rightarrow d$ transition, while Na does

not, this makes K more electronegative than Na and leads to the inverse charge transfer. It should be noted that Rahm et al.⁵² have also performed a systematic study on electronegativity of all the elements under pressure, who find that Na is the most electronegative element in the alkali metals. This is at odds with Dong's results. As described by the authors, this discrepancy may arise from different electronegativity definition, model construction or level of theory. The present Na-K system corresponds to the Dong's model which has also been mentioned in Ref [35].

Furthermore, we also calculate the electron-localization function (ELF) to characterize the atomic bonding. As shown in Figure 2e, at 10 GPa, the ELF basins surround the Na and K atoms correspond to the core electrons. Between the Na and K atoms, the ELF values are less than 0.5, which is typical for ionic and metallic bonding. We also observe ELF maximums (> 0.5)—usually represent interstitial electron localization—situated in the tetrahedral interstitial sites around Na atoms. As pressure increases, the ELF maximums disappear gradually, indicating that the interstitial electron localization is suppressed by pressure (Figure 2f and g). This is in contrast to elemental alkalis, wherein compression would increase interstitial electron localization due to the core-valence overlap⁵³⁻⁵⁶. This phenomenon has also been found by Frost et al.,³⁶ who explained that the reduced localization with pressure is due to the pressure-induced decrease sizes of interstitial spaces, and they inferred that it may reappear at higher pressures if this system remains stable. However, our calculations show that although NaK is stable under high pressure, no such electron localizations are found neither in the $Fd\bar{3}m$ phase at 300 GPa (Figure 2f) nor $Ibmm$ at 500 GPa (Figure 2g).

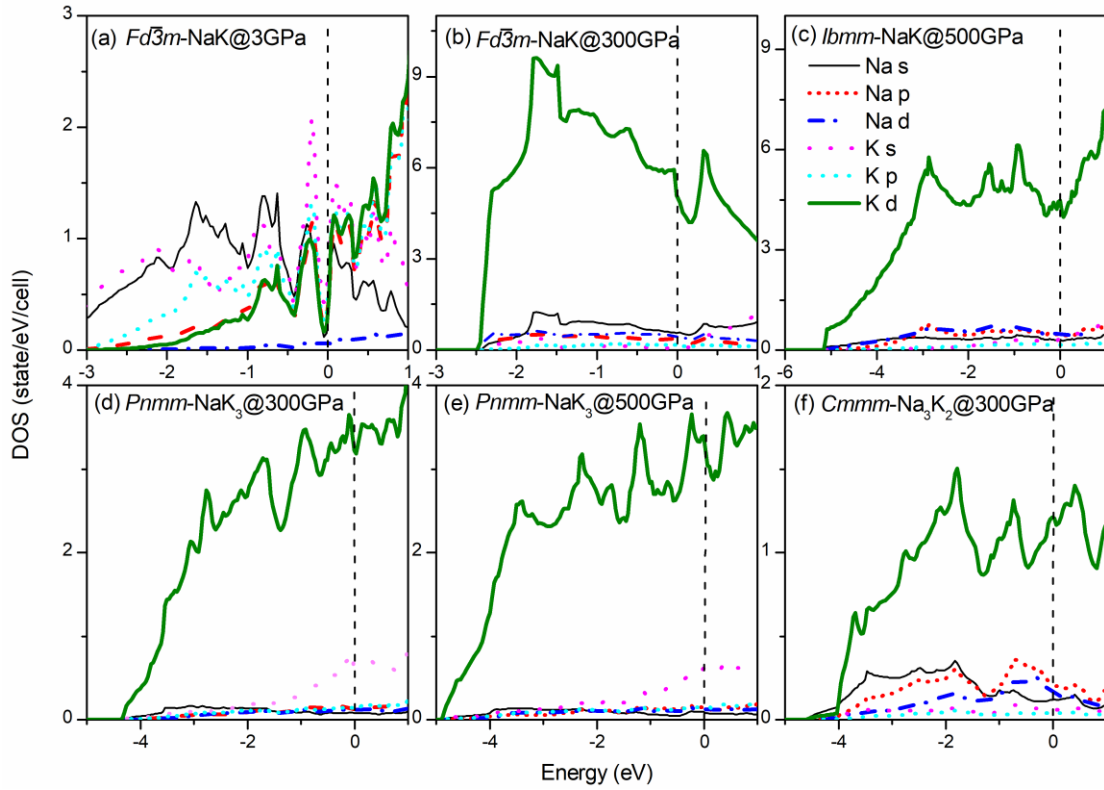


Figure 4. Calculated total and projected density of states of (a) $Fd\bar{3}m$ NaK at 3 GPa, (b) $Fd\bar{3}m$ NaK at 300 GPa, (c) $Ibmm$ NaK at 500 GPa, (d, e) $Pnmm$ NaK₃ at 300 and 500 GPa and (f) $Cmmm$ Na₃K₂ at 300 GPa.

Figure 4a-c display the calculated electronic density of states (DOS) for NaK at selected pressures. It is apparent that all the DOS results reveal metallic nature of NaK. For $Fd\bar{3}m$ NaK at 3 GPa, the states around the Fermi level are mainly contributed by the s and p orbitals of Na and K, and also have significant K- d contribution. As pressure increases, the K- d contribution becomes dominated (Figure 4b). This is expected since the pressure-induced $s \rightarrow d$ transition is common in K element^{17, 52}. At 500 GPa, the DOS of $Ibmm$ phase is analogously, wherein the K- d orbital contributes dominantly to the states around the Fermi level. It is interesting to note that the DOS of $Fd\bar{3}m$ NaK at low pressures is characterized by a pronounced pseudogap in the vicinity of Fermi level (Figure 4a). This pseudogap does not present at high pressures (see Figure 4b and c).

The appearance of pseudogap may be attributed to the localized electrons in the interstitial.

NaK₃ is predicted to crystallize in a Cu₃Ge-type structure (space group *Pnmm*) with 2 formula units per unit cell, consisting of K-sharing 12-fold NaK₁₂ icosahedron (Figure 2c). As is evidenced by the large DOS at the Fermi level (Figure 4d and e), this compound is a typical metallic alloy. Both at 300 and 500 GPa, the states around the Fermi level show large components of K-*d* contribution. The distances of neighboring Na-Na, Na-K and K-K distances are 3.19, 2.15 and 2.18 Å at 300 GPa, respectively. Given that the atomic radii of Na and K are, respectively, 1.18 and 1.23 Å, at 300 GPa,⁵⁷ the core-core overlaps in neighboring Na-K and K-K would take place. As a results, the dispersions of semi-core bands of K 3*s* and 3*p* are increased obviously (see Figure S3). It is well known that such core-core overlap is common in materials under high pressures, which plays an important role in their stability^{2, 21, 56, 58-59}. The ELF results (Figure 2h) indicate that the main interactions in this system are ionic and metallic.

In the case of Na₃K₂, it stabilizes in a *Cmmm* structure (Figure 2d) at 300 GPa and decomposes into NaK and K at 500 GPa. In *Cmmm* Na₃K₂, both Na and K are 8-coordinated. Each K is coordinated to 8 Na atoms and each Na to 4 K and 4 Na atoms. Na₃K₂ is also metallic with large value of DOS at the Fermi level contributed dominantly from the K-*d* states (Figure 4f). Comparing the atomic distances (the nearest neighboring Na-Na, Na-K and K-K distances are 1.96, 2.13 and 2.09 Å, respectively) with sums of atomic radii of Na and K at 300 GPa indicates that the core-core overlap also occurs in this system. In contrast to NaK₃, the ELF plot of Na₃K₂ indicates strong

interstitial electron localization (Figure 2i). Bader charge analysis also confirms this conclusion, which reveals that the charges of Na, K atoms and the interstitial sites are approximately 0.6, -0.5 and -0.9 respectively at 300 GPa, indicating that the electrons delocalized at the interstitial sites are mainly transferred from Na. These results demonstrate that Na_3K_2 is an electride compound in term of $\text{Na}_3\text{K}_2(e)$.

■ CONCLUSIONS

In summary, the swarm-intelligence structure-searching method is employed to explore the stability of Na-K system under high pressure. Three stoichiometries of NaK, NaK_3 and Na_3K_2 are found to form ground-state compounds under different pressures. NaK within the $Fd\bar{3}m$ structure is identified to stabilize at 5 - 35 GPa, and becomes unstable upon decomposition into Na and K above this pressure. When pressure further increase to 500 GPa, NaK restabilizes in a $Ibmm$ phase. The most K rich compound NaK_3 stabilizes in a Cu_3Ge -type structure at 300 - 500 GPa. Na_3K_2 is predicted to crystallize in a $Cmmm$ structure at 300 GPa and decomposes into NaK and K at 500 GPa. Remarkable pressure-induced charge-transfer reversal between Na and K atoms are revealed in these systems. Our results will deepen the understanding of interelectronic interactions of metals and stimulate future experimental and theoretical investigations.

■ ASSOCIATED CONTENT

Supporting Information.

Structure details, Phonon spectrums, Bader charge, Projected DOS, Pressure dependent enthalpies of formation of NaK, NaK_3 and Na_3K_2 .

■ AUTHOR INFORMATION

Corresponding Authors

* E-mail: xzyan01@qq.com.

* E-mail: s102genghy@caep.ac.cn.

Notes

The authors declare no competing financial interests.

■ ACKNOWLEDGMENT

This work is supported by the National Natural Science Foundation of China under Grant nos. 11704163, 11672274, 11804131, and 11274281, the CAEP Research Projects under Grant nos. 2012A0101001 and 2015B0101005, the NSAF under Grant no. U1730248, the Fund of National Key Laboratory of Shock Wave and Detonation Physics of China under Grant no. 6142A03010101, the China Postdoctoral Science Foundation under Grant no. 2017M623064, the Natural Science Foundation of Jiangxi Province of China under Grant no. 20181BAB211007 and the PhD research startup foundation of Jiangxi University of Science and Technology under Grant nos. 3401223301, 3401223256. This work is supported by the National Natural Science Foundation of China (11804131, 11704163, 11672274 and 11404006), the Science challenge Project (TZ2016001), the CAEP Research Project (CX2019002), the NSAF (U1730248), the Science challenge Project (TZ2016001), the CAEP Research Project (CX2019002), the China Postdoctoral Science Foundation (2017M623064), the Natural Science Foundation of Jiangxi Province of China (20181BAB211007), and the Ph.D. research startup foundation of Jiangxi University of Science and Technology

(3401223301 and 3401223256), the Scientific Research Fund of Jiangxi Provincial Education Department (Grant No.GJJ160594).

■ REFERENCES

- (1) Hanfland, M.; Syassen, K.; Christensen, N.; Novikov, D., New High-Pressure Phases of Lithium. *Nature* **2000**, *408*, 174-178.
- (2) Ma, Y.; Eremets, M.; Oganov, A. R.; Xie, Y.; Trojan, I.; Medvedev, S.; Lyakhov, A. O.; Valle, M.; Prakapenka, V., Transparent Dense Sodium. *Nature* **2009**, *458*, 182-185.
- (3) Ma, Y.; Oganov, A. R.; Xie, Y., High-Pressure Structures of Lithium, Potassium, and Rubidium Predicted by an Ab Initio Evolutionary Algorithm. *Phys. Rev. B* **2008**, *78*, 014102.
- (4) Gregoryanz, E.; Lundegaard, L. F.; McMahon, M. I.; Guillaume, C.; Nelmes, R. J.; Mezouar, M., Structural Diversity of Sodium. *Science* **2008**, *320*, 1054-1057.
- (5) Rousseau, B.; Xie, Y.; Ma, Y.; Bergara, A., Exotic High Pressure Behavior of Light Alkali Metals, Lithium and Sodium. *Eur. Phys. J. B* **2011**, *81*, 1.
- (6) McMahon, M.; Nelmes, R.; Schwarz, U.; Syassen, K., Composite Incommensurate K-Iii and a Commensurate Form: Study of a High-Pressure Phase of Potassium. *Phys. Rev. B* **2006**, *74*, 140102.
- (7) McMahon, M.; Rekhi, S.; Nelmes, R., Pressure Dependent Incommensuration in Rb-Iv. *Phys. Rev. Lett.* **2001**, *87*, 055501.
- (8) Nelmes, R.; McMahon, M.; Loveday, J.; Rekhi, S., Structure of Rb-Iii: Novel Modulated Stacking Structures in Alkali Metals. *Phys. Rev. Lett.* **2002**, *88*, 155503.
- (9) McMahon, M. I.; Nelmes, R. J., High-Pressure Structures and Phase Transformations in Elemental Metals. *Chem. Soc. Rev.* **2006**, *35*, 943-963.
- (10) Hanfland, M.; Loa, I.; Syassen, K., Sodium under Pressure: Bcc to Fcc Structural Transition and Pressure-Volume Relation to 100 GPa. *Phys. Rev. B* **2002**, *65*, 184109.
- (11) Olijnyk, H.; Holzapfel, W., Phase Transitions in K and Rb under Pressure. *Phys. Lett. A* **1983**, *99*, 381-383.
- (12) Fabbris, G.; Lim, J.; Veiga, L.; Haskel, D.; Schilling, J., Electronic and Structural Ground State of Heavy Alkali Metals at High Pressure. *Phys. Rev. B* **2015**, *91*, 085111.
- (13) Degtyareva, V. F., Simple Metals at High Pressures: The Fermi Sphere–Brillouin Zone Interaction Model. *Physics-Uspekhi* **2006**, *49*, 369.
- (14) Boettger, J.; Trickey, S., Equation of State and Properties of Lithium. *Phys. Rev. B* **1985**, *32*, 3391.
- (15) Skriver, H. L., Crystal Structure from One-Electron Theory. *Phys. Rev. B* **1985**, *31*, 1909.
- (16) Boettger, J.; Albers, R., Structural Phase Stability in Lithium to Ultrahigh Pressures. *Phys. Rev. B* **1989**, *39*, 3010.
- (17) McMahan, A., Alkali-Metal Structures above the S– D Transition. *Phys. Rev. B* **1984**, *29*, 5982.

- (18) Shimizu, K.; Ishikawa, H.; Takao, D.; Yagi, T.; Amaya, K., Superconductivity in Compressed Lithium at 20 K. *Nature* **2002**, *419*, 597-599.
- (19) Struzhkin, V. V.; Eremets, M. I.; Gan, W.; Mao, H.-k.; Hemley, R. J., Superconductivity in Dense Lithium. *Science* **2002**, *298*, 1213-1215.
- (20) Schaeffer, A. M.; Temple, S. R.; Bishop, J. K.; Deemyad, S., High-Pressure Superconducting Phase Diagram of 6Li: Isotope Effects in Dense Lithium. *Proc. Natl. Acad. Sci.* **2015**, *112*, 60-64.
- (21) Guillaume, C. L.; Gregoryanz, E.; Degtyareva, O.; McMahon, M. I.; Hanfland, M.; Evans, S.; Guthrie, M.; Sinogeikin, S. V.; Mao, H., Cold Melting and Solid Structures of Dense Lithium. *Nature Phys.* **2011**, *7*, 211-214.
- (22) Feng, Y.; Chen, J.; Alfè, D.; Li, X.-Z.; Wang, E., Nuclear Quantum Effects on the High Pressure Melting of Dense Lithium. *J. Chem. Phys.* **2015**, *142*, 064506.
- (23) Marqués, M.; McMahon, M.; Gregoryanz, E.; Hanfland, M.; Guillaume, C.; Pickard, C.; Ackland, G.; Nelmes, R., Crystal Structures of Dense Lithium: A Metal-Semiconductor-Metal Transition. *Phys. Rev. Lett.* **2011**, *106*, 095502.
- (24) Lv, J.; Wang, Y.; Zhu, L.; Ma, Y., Predicted Novel High-Pressure Phases of Lithium. *Phys. Rev. Lett.* **2011**, *106*, 015503.
- (25) Matsuoka, T.; Shimizu, K., Direct Observation of a Pressure-Induced Metal-to-Semiconductor Transition in Lithium. *Nature* **2009**, *458*, 186-189.
- (26) Matsuoka, T.; Sakata, M.; Nakamoto, Y.; Takahama, K.; Ichimaru, K.; Mukai, K.; Ohta, K.; Hirao, N.; Ohishi, Y.; Shimizu, K., Pressure-Induced Reentrant Metallic Phase in Lithium. *Phys. Rev. B* **2014**, *89*, 144103.
- (27) Zhang, X.; Zunger, A., Altered Reactivity and the Emergence of Ionic Metal Ordered Structures in Li-Cs at High Pressures. *Phys. Rev. Lett.* **2010**, *104*, 245501.
- (28) Botana, J.; Miao, M.-S., Pressure-Stabilized Lithium Caesides with Caesium Anions Beyond the -1 State. *Nat. Commun.* **2014**, *5*, 4861.
- (29) Desgreniers, S.; John, S. T.; Matsuoka, T.; Ohishi, Y.; Justin, J. T., Mixing Unmixables: Unexpected Formation of Li-Cs Alloys at Low Pressure. *Sci. Advances* **2015**, *1*, e1500669.
- (30) Simon, A.; Ebbinghaus, G., Zur Existenz Neuer Verbindungen Zwischen Alkalimetallen/on the Existence of New Compounds between Alkali Metals. *Z. Naturforsch. B* **1974**, *29*, 616-618.
- (31) Chen, Y.-M.; Geng, H.-Y.; Yan, X.-Z.; Wang, Z.-W.; Chen, X.-R.; Wu, Q., Predicted Novel Insulating Electride Compound between Alkali Metals Lithium and Sodium under High Pressure. *Chin. Phys. B* **2017**, *26*, 056102.
- (32) Natesan, K.; Reed, C.; Mattas, R., Assessment of Alkali Metal Coolants for the Iter Blanket. *Fusion Eng. Des.* **1995**, *27*, 457-466.
- (33) Bale, C. W., The K-Na (Potassium-Sodium) System. *Bull. Alloy Phase Diagrams* **1982**, *3*, 313-318.
- (34) Zhu, M. J.; Bylander, D.; Kleinman, L., Multiatom Covalent Bonding and the Formation Enthalpy of Na₂K. *Phys. Rev. B* **1996**, *53*, 14058.
- (35) Yang, L.; Qu, X.; Zhong, X.; Wang, D.; Chen, Y.; Yang, J.; Lv, J.; Liu, H., Decomposition and Recombination of Binary Interalkali Na₂K at High Pressures. *J. Phys. Chem. Lett.* **2019**, *10*, 3006-3012.

- (36)Frost, M.; McBride, E. E.; Schörner, M.; Redmer, R.; Glenzer, S. H., Sodium-Potassium System at High Pressure. *Phys. Rev. B* **2020**, *101*, 224108.
- (37)Wang, Y.; Lv, J.; Zhu, L.; Ma, Y., Calypso: A Method for Crystal Structure Prediction. *Comput. Phys. Commun.* **2012**, *183*, 2063-2070.
- (38)Wang, Y.; Lv, J.; Zhu, L.; Ma, Y., Crystal Structure Prediction Via Particle-Swarm Optimization. *Phys. Rev. B* **2010**, *82*, 094116.
- (39)Gao, B.; Gao, P.; Lu, S.; Lv, J.; Wang, Y.; Ma, Y., Interface Structure Prediction Via Calypso Method. *Sci. Bull.* **2019**, *64*, 301-309.
- (40)Wang, Y.; Lv, J.; Zhu, L.; Lu, S.; Yin, K.; Li, Q.; Wang, H.; Zhang, L.; Ma, Y., Materials Discovery Via Calypso Methodology. *J. Phys.: Condens. Matter* **2015**, *27*, 203203.
- (41)Wang, H.; Wang, Y.; Lv, J.; Li, Q.; Zhang, L.; Ma, Y., Calypso Structure Prediction Method and Its Wide Application. *Comp. Mater. Sci.* **2016**, *112*, 406-415.
- (42)Li, Y.; Wang, Y.; Pickard, C. J.; Needs, R. J.; Wang, Y.; Ma, Y., Metallic Icosahedron Phase of Sodium at Terapascal Pressures. *Phys. Rev. Lett.* **2015**, *114*, 125501.
- (43)Chen, Y.; Geng, H. Y.; Yan, X.; Sun, Y.; Wu, Q.; Chen, X., Prediction of Stable Ground-State Lithium Polyhydrides under High Pressures. *Inorg. Chem.* **2017**, *56*, 3867-3874.
- (44)Kresse, G.; Furthmüller, J., Software Vasp, Vienna (1999); *Phys. Rev. B*, 1996, *54*, 11169. *Comput. Mater. Sci.* **1996**, *6*, 15.
- (45)Perdew, J. P.; Burke, K.; Ernzerhof, M., Generalized Gradient Approximation Made Simple. *Phys. Rev. Lett.* **1996**, *77*, 3865.
- (46)Togo, A.; Oba, F.; Tanaka, I., First-Principles Calculations of the Ferroelastic Transition between Rutile-Type and CaCl₂-Type SiO₂ at High Pressures. *Phys. Rev. B* **2008**, *78*, 134106.
- (47)Ackland, G. J.; Macleod, I. R., Origin of the Complex Crystal Structures of Elements at Intermediate Pressure. *New J. Phys.* **2004**, *6*, 138-138.
- (48)Ma, Y.; Oganov, A. R.; Xie, Y., High-Pressure Structures of Lithium, Potassium, and Rubidium Predicted by Anab Initioevolutionary Algorithm. *Phys. Rev. B* **2008**, *78*.
- (49)McMahon, M. I.; Nelmes, R. J.; Schwarz, U.; Syassen, K., Composite Incommensurate K-Iii and a Commensurate Form: Study of a High-Pressure Phase of Potassium. *Phys. Rev. B* **2006**, *74*, 140102.
- (50)Lundegaard, L. F.; Marqués, M.; Stinton, G.; Ackland, G. J.; Nelmes, R. J.; McMahon, M. I., Observation of the Op8 Crystal Structure in Potassium at High Pressure. *Phys. Rev. B* **2009**, *80*, 020101.
- (51)Dong, X.; Oganov, A. R.; Qian, G.; Zhou, X.-F.; Zhu, Q.; Wang, H.-T., How Do Chemical Properties of the Atoms Change under Pressure. *arXiv preprint arXiv:1503.00230* **2015**.
- (52)Rahm, M.; Cammi, R.; Ashcroft, N. W.; Hoffmann, R., Squeezing All Elements in the Periodic Table: Electron Configuration and Electronegativity of the Atoms under Compression. *J. Am. Chem. Soc.* **2019**, *141*, 10253-10271.
- (53)Miao, M. s.; Hoffmann, R.; Botana, J.; Naumov, I. I.; Hemley, R. J., Quasimolecules in Compressed Lithium. *Ange. Chem.* **2017**, *129*, 992-995.

- (54) Naumov, I. I.; Hemley, R. J.; Hoffmann, R.; Ashcroft, N., Chemical Bonding in Hydrogen and Lithium under Pressure. *J. Chem. Phys.* **2015**, *143*, 064702.
- (55) Miao, M. S.; Hoffmann, R., High-Pressure Electrides: The Chemical Nature of Interstitial Quasiatoms. *J. Am. Chem. Soc.* **2015**, *137*, 3631-7.
- (56) Miao, M. S.; Hoffmann, R., High Pressure Electrides: A Predictive Chemical and Physical Theory. *Acc. Chem. Res.* **2014**, *47*, 1311-7.
- (57) Rahm, M.; Ångqvist, M.; Rahm, J. M.; Erhart, P.; Cammi, R., Non-Bonded Radii of the Atoms under Compression. *Chem. Phys. Chem.* **2020**, *21*, 2441-2453.
- (58) Pickard, C. J.; Needs, R. J., Aluminium at Terapascal Pressures. *Nat. Mater.* **2010**, *9*, 624-627.
- (59) Grochala, W.; Hoffmann, R.; Feng, J.; Ashcroft, N. W., The Chemical Imagination at Work in Very Tight Places. *Angew. Chem. Int. Edit.* **2007**, *46*, 3620-3642.

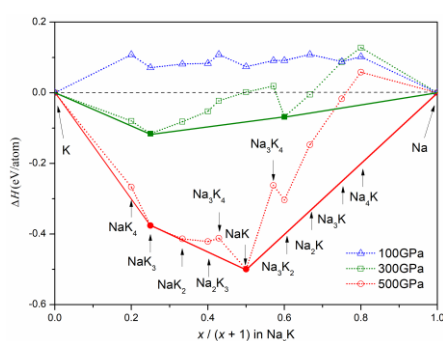


Table of contents (TOC) graphic: Chemical stabilities of Na-K system with respect to elemental Na and K at different pressures. The compounds of NaK, NaK_3 and Na_3K_2 are predicted to be stable under different pressures.

Supporting Information for “Prediction of Stable Ground-State Binary Sodium-Potassium Interalkalis under High Pressures”

Yangmei Chen¹, Xiaozhen Yan^{1,2}, Huayun Geng*², Xiaowei Sheng³, Leilei Zhang²,*

Hao Wang², Jinglong Li², Ye Cao,² and Xiaolong Pan²

1. School of Science, Jiangxi University of Science and Technology, Ganzhou

341000, Jiangxi, People’s Republic of China

2. National Key Laboratory of Shock Wave and Detonation Physics, Institute of

Fluid Physics, CAEP, P.O. Box 919-102, Mianyang 621900, Sichuan, People’s

Republic of China

3. Department of Physics, Anhui Normal University, Anhui 241000, Wuhu, People’s

Republic of China

Corresponding Author

* Xiaozhen Yan: xzyan01@qq.com.

* Huayun Geng: s102genghy@caep.cn.

Auxiliary Table S1. Structure details of the conventional unit cell of NaK, NaK₃ and Na₃K₂ from the CALYPSO structure searches at different pressures.

Phase	Pressure (GPa)	Space group	Lattice parameters	Atomic coordinates
NaK	10	$\bar{F}d\bar{3}m$	a = b = c = 6.7242 Å	Na(8a) 0.75 -0.25 0.25
			$\alpha = \beta = \gamma = 90.000^\circ$	K(8b) 0.25 -0.25 0.25
NaK	500	<i>Ibmm</i>	a = 5.0839 Å	Na(8h) -0.50 0.03 -0.70
			b = 4.2379 Å	K(8i) -0.71 0.75 -0.98
			c = 4.4169 Å	
			$\alpha = \beta = \gamma = 90.000^\circ$	
NaK ₃	300	<i>Pnmm</i>	a = 3.4771 Å	Na(2b) 0.50 0.00 -0.32
			b = 4.4920 Å	K1(4e) 0.50 0.75 -0.83
			c = 3.9227 Å	K2(2a) 0.50 0.50 -0.35
			$\alpha = \beta = \gamma = 90.000^\circ$	
Na ₃ K ₂	300	<i>Cmmm</i>	a = 3.2827 Å	Na1(4j) 0.00 0.89 0.50
			b = 10.2332 Å	Na3(2c) 0.50 0.00 0.50
			c = 2.1409 Å	K1(4i) 0.50 0.81 0.00
			$\alpha = \beta = \gamma = 90.000^\circ$	

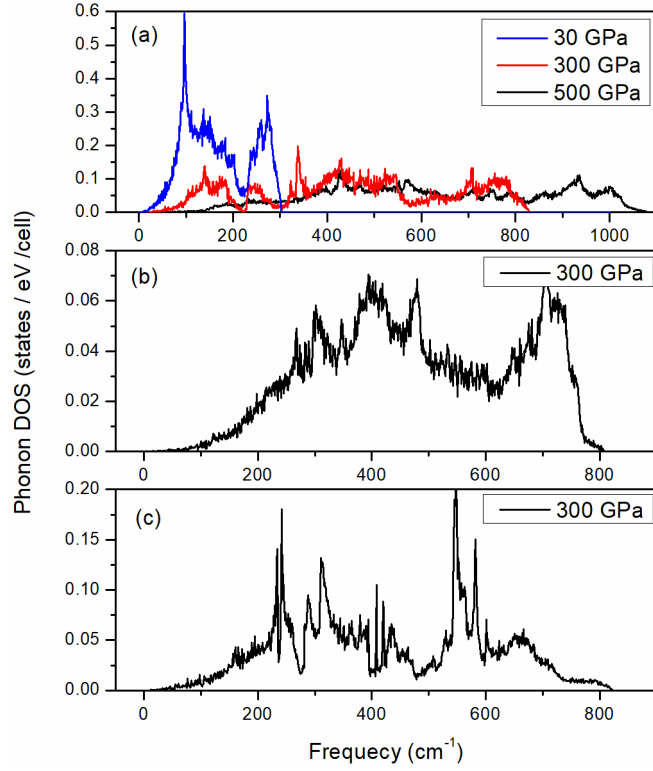


Figure S1. Phonon spectrums of (a) $Fd \bar{3}m$ NaK at 30 GPa, 300 GPa and $Ibmm$ NaK at 500 GPa, (b) $Pnmm$ NaK₃ at 300 GPa, (c) $Cmmm$ Na₃K₂ at 300 GPa.

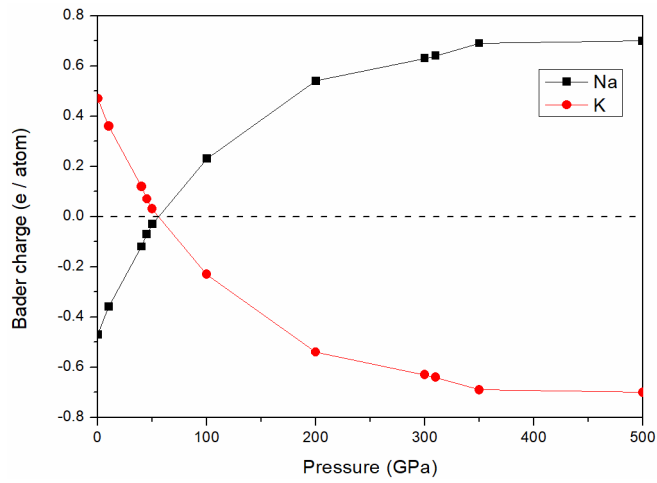


Figure S2. Bader charge of Na and K in NaK. Positive/negative value corresponds to loss/gain of electron.

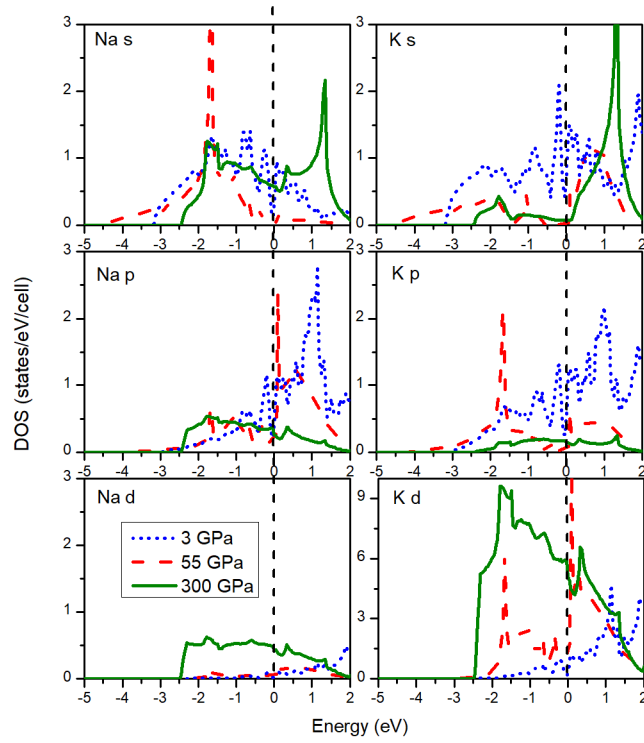


Figure S3. Pressure dependence of projected electronic DOS $Fd \bar{3}m$ NaK. The zero of energy is placed at the Fermi energy.

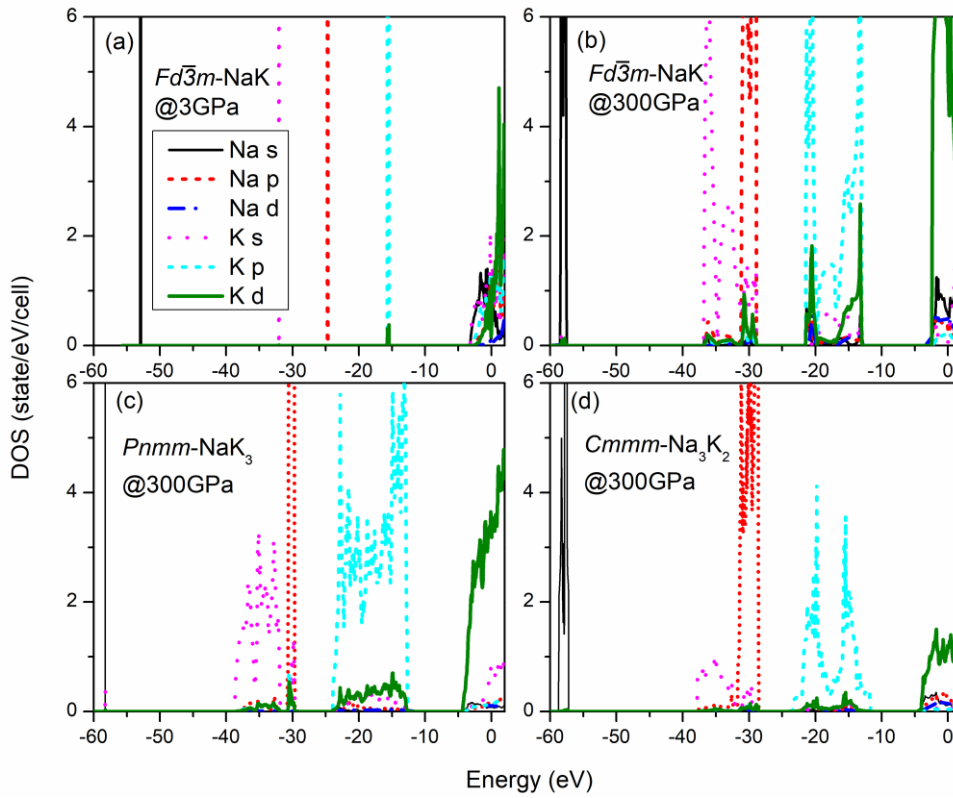


Figure S4. Projected electronic DOS showing the Na 2s, Na 2p, K 3s and K 3p

semi-core states and the valence states. The zero of energy is placed at the Fermi energy.

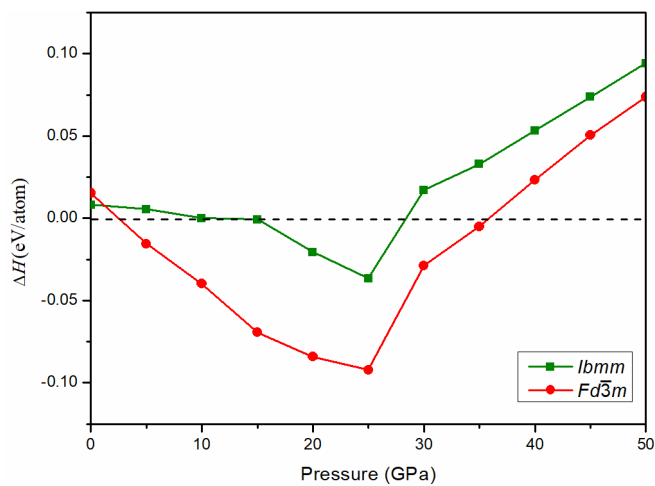


Figure S5. Enthalpies of formation of NaK with respect to decomposition into Na and K at 0 - 50 GPa.

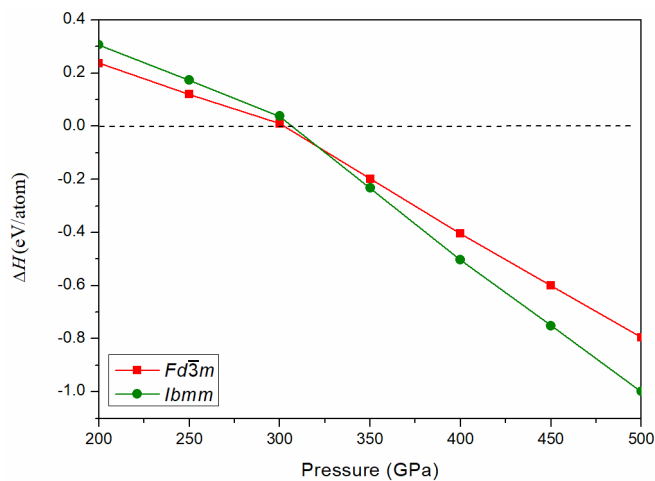


Figure S6. Enthalpies of formation of NaK with respect to decomposition into Na and K at 200 - 500 GPa.

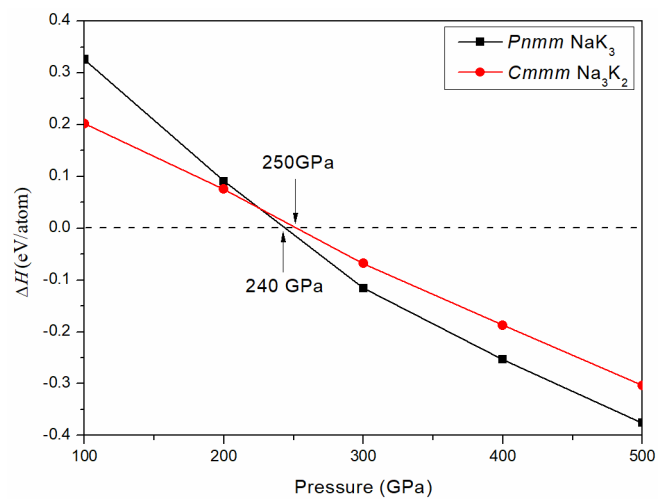


Figure S7. Enthalpies of formation of NaK_3 and Na_3K_2 with respect to decomposition into Na and K at 100 - 500 GPa.